Article:
Zhou, X., Chen, Q., Feng, W. et al. (Accepted: 2026) Residence time of Hunga stratospheric water vapour perturbation quantified at 9 years. Communications Earth & Environment. (In Press)

https://doi.org/10.1038/s43247-026-03216-5

Communications Earth & Environment https://doi.org/10.1038/s43247-026-03216-5

Article in Press

Residence time of Hunga stratospheric water vapour perturbation quantified at 9 years

Received: 5 September 2025

Accepted: 12 January 2026

Cite this article as: Zhou, X., Chen, Q., Feng, W. *et al.* Residence time of Hunga stratospheric water vapour perturbation quantified at 9 years. *Commun Earth Environ* (2026). https://doi.org/10.1038/s43247-026-03216-5

Xin Zhou, Quanliang Chen, Wuhu Feng, Saffron Heddell, Sandip S. Dhomse, Graham Mann, Hugh C. Pumphrey, Luis Millán, Michelle L. Santee & Martyn P. Chipperfield

Residence time of Hunga stratospheric water vapour perturbation quantified at 9 years

Xin Zhou[1,2*], Quanliang Chen[1], Wuhu Feng[2,3], Saffron Heddell[2], Sandip S. Dhomse[2,4], Graham Mann[2], Hugh C. Pumphrey[5], Luis Millán[6], Michelle L. Santee[6], Martyn P. Chipperfield[2,4]

[1*]School of Atmospheric Sciences, Chengdu University of Information Technology, Chengdu, 610225, China.
[2]School of Earth and Environment, University of Leeds, Leeds, LS2 9JT, UK.
[3]National Centre for Atmospheric Science, University of Leeds, Leeds, LS2 9PH, UK.
[4]National Centre for Earth Observation, University of Leeds, Leeds, LS2 9JT, UK.
[5]School of GeoSciences, University of Edinburgh, Edinburgh, EH8 9XP, UK.
[6]Jet Propulsion Laboratory, California Institute of Technology, Pasadena, USA.

*Corresponding author(s). E-mail(s): x.zhou1@leeds.ac.uk;

Abstract

The January 2022 eruption of the Hunga volcano (20°S) injected 150 Tg of water vapour into the middle atmosphere, leading to an increase in the stratospheric water burden of 10%, unprecedented in the observational record. In the first two years post eruption the stratospheric burden hardly changed, leaving the residence time of volcanically injected water vapour, a key control on its climate impact, uncertain. Here, using satellite observations, we show a substantial decline from 2024 to early 2025, the largest drop since the eruption. Comparison with 3-D numerical model simulations shows that the long-term removal of the Hunga water has now entered a new phase, with stratosphere-troposphere exchange playing an increasingly important role, exceeding Antarctic dehydration in 2024. We estimate that the additional stratospheric water vapour is now decaying steadily with an e-folding time of 3 years and will reach the observed pre-Hunga range of variability around 2030.

Keywords: Hunga eruption, stratospheric water vapour, residence time, stratosphere-troposphere exchange

Introduction

Water vapour, as one of the most prominent greenhouse gases [1], can effectively alter radiative forcing and influence global surface temperature once it enters the stratosphere [2]. In January 2022, the underwater volcanic eruption of Hunga injected a huge amount (∼150 Tg) of water vapour (Fig. 1) and a moderate amount (∼0.5 Tg) of sulfur dioxide (SO_2) into the stratosphere and lower mesosphere, leading to an instantaneous increase in the global stratospheric water mass of ∼10% [3]. This is the largest stratospheric perturbation of water vapour observed in the satellite era spanning more than 30 years. The eruption impacted stratospheric chemistry [4–7] and dynamics [8–11] and challenged preconceptions about volcanic climate impacts [12–14].

Despite its critical importance for accurately predicting the near-term climate impact, estimating how long the Hunga-injected excess stratospheric water (HEW) will persist has been challenging. The major sinks of stratospheric water vapour are ice polar stratospheric cloud (PSC) sedimentation [15] and stratosphere-to-troposphere transport in middle-to-high latitudes [16], with additional small loss in the mesosphere due to photolysis [17]. Although Antarctic PSCs removed around 12 Tg more water vapour in the 2023 austral winter than typical, the overall amount of stratospheric water vapour mass increased again and recovered to ∼135 Tg (above 2005–2021 climatology) in late 2023 [18] due to a larger-than-usual amount of water vapour entering the stratosphere via the tropical troposphere [19]. Up to now, there has been a large uncertainty in the estimation of residence time of HEW in the stratosphere, with the projections of its return to pre-Hunga conditions ranging from as early as 2025 (over 3 years [20]) to more than a decade [19]. Chemistry-climate model simulations in the Hunga Model–Observation Comparison (HTHH–MOC) free-running experiment also show a wide range in their simulated recovery times (green bar in Fig. 4b) [21].

The Microwave Limb Sounder (MLS) on board NASA's Aura satellite [22] has continuously observed HEW (estimated by comparison with pre-Hunga climatology). We now have sufficient observations to characterise the decay of the Hunga water. For the first time, we are able to reduce the uncertainty substantially by showing the decay of HEW using daily near-global profiles and interpreting the observed changes using a model.

Results

1 A sudden severe drop in 2024

In 2024, a sudden severe drop is observed by MLS, rapidly reducing HEW by ∼55 Tg within just one year (Fig. 1). This abrupt drop is the largest and fastest in the past 30 years, exceeding the previous two drops in satellite records, i.e., the millennium

drop during 2001–2005 [2, 23] and 2012–2013 [24]. These two prior events saw similar reductions of ∼40 Tg (∼0.4 ppmv in the global average) and were both driven by decreases in the tropical entry value of water vapour. The persistent drop in 2024 signals a change in the behaviour of the excess Hunga H_2O, leaving the initial injection diminished by nearly half at the end of 2024.

We performed calculations with the TOMCAT [25] offline 3-D chemical transport model, forced by ERA5 [26] meteorological fields. TOMCAT includes the time-varying stratospheric transport and temperature-dependent PSC onset that is important for the settling of ice particles. The model has been shown to reliably capture the spread and dehydration of HEW through late 2023 [19].

Two pairs of model simulations, using detailed stratospheric chemistry, were used to simulate the transport of HEW, examine the drivers of its changes, and predict its residence time (see Supplementary Table 1). The first pair included a simulation representing the Hunga injection of water vapour and a corresponding control run without the injection, allowing examination of the evolution of HEW by removing the background variations. The second pair was similar but excluded PSC dehydration loss in both simulations. The comparison between the two pairs was used to quantify the varying contributions of PSC dehydration and stratosphere-troposphere exchange (STE) to the decay of HEW. The height and amount of the volcanic injection, including aerosol and gas-phase water, were based on satellite observations. Further information on methods, data sets, and the model is provided in Section 5.

The model reproduces well the observed persistent drop in HEW through the year 2024, as well as the previous near-instantaneous decline in 2023 Antarctic winter, demonstrating its skill in representing the removal pathways for stratospheric water vapour. The rapid increase due to the additional tropical entry in late 2023 was not captured as the model uses a fixed repeating seasonal cycle of the tape recorder signal [27] for the tropical entry. However, the model is still able to represent the transport of HEW, unaffected by the changes in the background level. This is important as it allows us to use sensitivity experiments to quantify the dehydration pathways of the Hunga water by isolating it from the moistening background [18].

2 Explaining the observed Hunga water changes

Every year in June to mid-August, Antarctic PSC dehydration efficiently removes a large amount (∼23 Tg) of water vapour from the stratosphere [18]. In 2022, the Hunga water was excluded from the Antarctic polar vortex as it arrived later than the formation of the strong polar vortex [28]. However, in 2023, the strongest dehydration (35 Tg) in the satellite observational record occurred in late May to August[18, 19, 29, 30], explaining the majority of the HEW loss at that time (the grey bars in Fig. 1).

In contrast, the observed 2024 drop in HEW is persistent throughout the year (the orange shading period in Fig. 1), with only a moderate amount of anomalous Antarctic PSC loss. The Antarctic H_2O anomaly in the lower stratosphere returns to essentially zero (Fig. 2b), like 2023 and previous years, as the vortex humidity is controlled by the local polar temperatures [19, 29]. The water remaining in the gas phase is determined by its saturation vapour pressure; the ice particles that form and

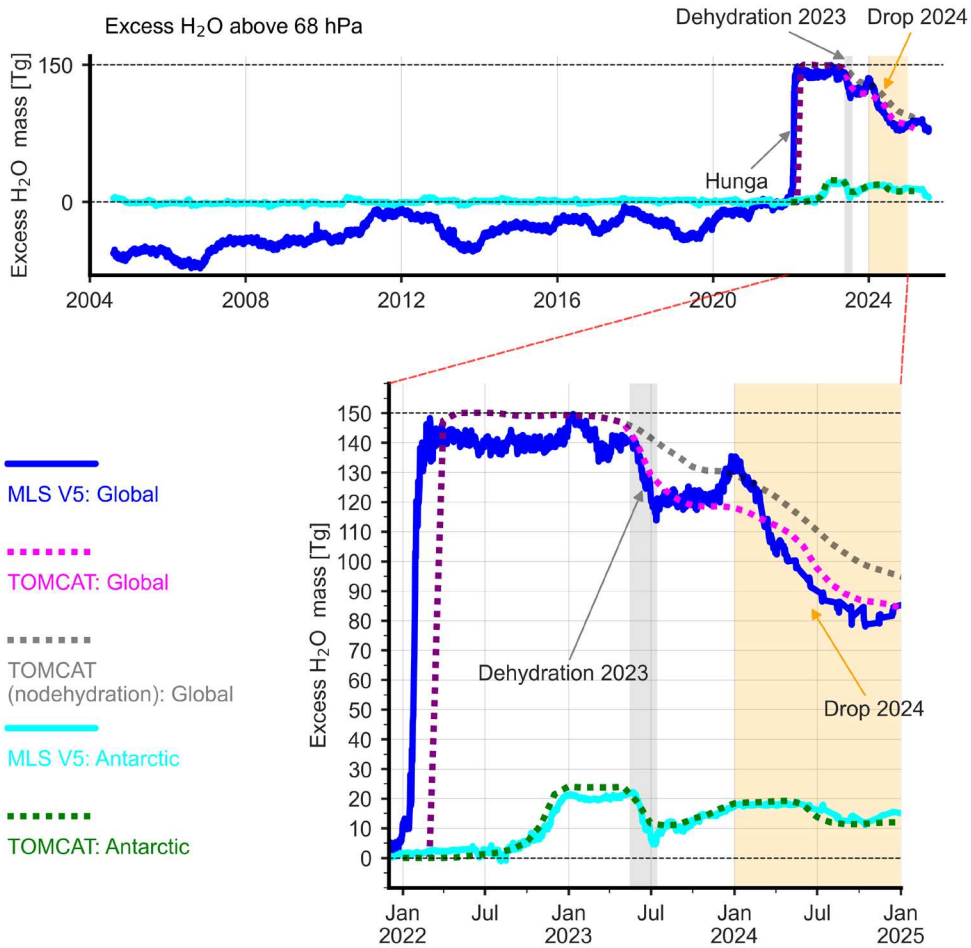

Fig. 1: **Stratospheric water excess mass following the Hunga eruption.** The top panel shows the full time series (2004-2025) of both global (blue: MLS daily observations; magenta: TOMCAT model monthly simulations) and Antarctic polar cap (cyan: MLS; green: TOMCAT) stratospheric water vapour mass anomalies. The bottom panel provides a zoomed-in view of the post-eruption changes from 2022 through 2024. The grey bar marks the months of June and July 2023. The orange shading marks the year 2024. The grey dotted line represents the TOMCAT simulation without dehydration processes. The stratospheric water mass is calculated for pressure levels above (i.e., pressures lower than) 68 hPa. MLS daily anomalies are obtained by removing the 2005–2021 climatology. Note that the TOMCAT simulation has increased water vapour from April 2022. See Methods for more details.

sediment out in austral winter permanently remove the condensed water vapour from the stratosphere. This mechanism is not affected by the HEW. However, in 2024, the Antarctic polar vortex is not as moist as it was in the previous year (Fig. 2a,b), as Hunga water had spread globally via the stratospheric circulation. Accordingly, the amount of HEW removed by Antarctic PSC dehydration in 2024 is not as large as that in 2023, although it still exceeds the climatological mean seasonal dehydration by ∼6 Tg (cyan line in Fig. 1; see also the total amount of dehydration in Supplementary Fig. 1).

Formation of ice PSCs in Arctic winters, and subsequent dehydration, is relatively uncommon compared to Antarctica; the Arctic polar vortex is usually warmer than its Antarctic counterpart and has larger variability, with frequent exchange of cold air within the polar vortex and warm air at lower latitudes. Only in very cold winters, such as those of 2009–2010 [31], 2012–2013 [32], 2015–2016 [33], and 2019–2020 [34], do observations show that Arctic PSC dehydration occurred for a short period of time. Winter 2023–2024 was the first when the Hunga excess water reached the Arctic, with the polar-cap-averaged anomalous humidity being ∼1 ppmv, larger than that in any other year since 2004 (Fig. 2d). However, the 2023–2024 Arctic vortex was weaker, warmer, and more dynamically disturbed than typical Arctic winters [35, 36]. As a result, strong descent of HEW to the lower stratosphere was observed (Fig. 2c), but no substantial PSC dehydration was detected. The 2024–2025 boreal winter was much colder than the previous one, with temperatures below the frost point in late January 2025. Consequently, a signature of Arctic dehydration is observed by MLS in the first half of January 2025 (red line in Fig. 2d) and simulated by the model (Fig. 3c). The impact of this on the overall mass of stratospheric Hunga water is, however, modest (∼1 Tg, Fig. 3c).

The evolution of HEW entered a new phase in 2024 when the majority of its removal was no longer attributable to polar dehydration. While much of HEW had been confined above 25 km [18, 19, 37, 38], the global stratospheric circulation has now resulted in downward transport of HEW over middle and high latitudes. In each winter, the strong descent of mid-stratospheric air parcels near the poles [39], via descending branch of the Brewer-Dobson circulation (BDC), is accompanied by the downward migration of stratospheric tracers, such as ozone and H_2O. This downward migration of the Hunga water vapour is observed by MLS and is well captured in the TOMCAT *Hunga* simulation (Fig. 3a).

Since late 2023, a large mass fraction (∼18%; Fig. 3b) of the Hunga water vapour has been transported to the lower stratosphere below 100 hPa, where it is subject to irreversible stratosphere-to-troposphere transport. During the 2023–2024 boreal winter, two major sudden stratospheric warmings occurred, accompanied by stronger-than-usual descent relative to the climatology [36]. This led to a rapid downward migration of HEW during this period (Fig. 2c; see also Supplementary Fig.2). The 2024 austral winter was also anomalously warm, with large amount of strongly moistened air descending below 100 hPa over May to July in the mid-to-high latitudes of the Southern Hemisphere (Supplementary Fig.2). This enhanced descent of HEW in both hemispheres caused the subsequent decay via STE. The transport-induced decay has two pathways: 1) stratospheric air with Hunga-injected H_2O slowly descends

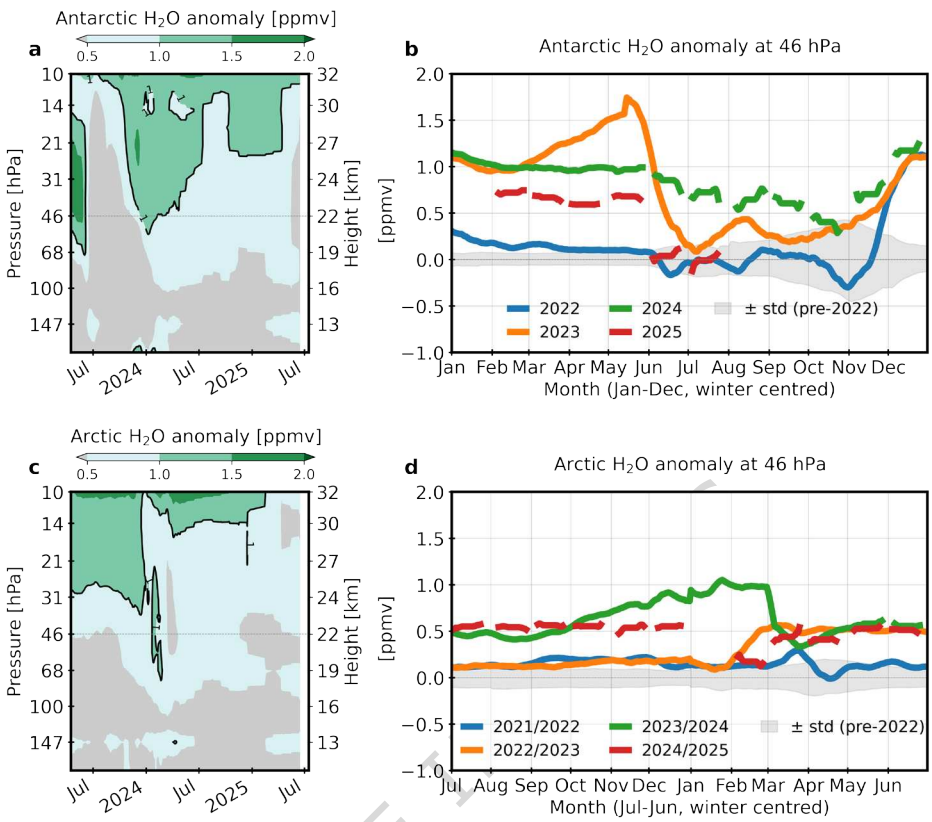

Fig. 2: **MLS-observed dehydration of the Antarctic and Arctic polar regions.** (a, b) Pressure-time cross-section for daily water vapour mixing ratio anomalies averaged over the (a) Antarctic (60-90°S) and (c) Arctic (60-90°N). Contours in panels (a) and (c) show 1 ppmv anomaly as an indication for the Hunga plume. (b) Time series of Antarctic H_2O anomalies at 46 hPa (within the PSC layer), showing data from each year starting from January. (d) Time series of Arctic H_2O anomalies at 46 hPa, with the timeline starting from July through June to centre the Arctic winter season (December–January–February). Anomalies are calculated by removing climatology for 2005-2021, with a 15-day smoothing to minimize the gaps present in the MLS data since April 2024. The ±1 standard deviation is provided in panels (b) and (d) as a measure for the internal variability.

into the troposphere at high latitudes via the deep branch of the BDC; 2) vigorous stratospheric intrusions in the mid latitudes led to transport of Hunga-moistened stratospheric air into the troposphere. These processes permanently remove HEW from the stratosphere. We now examine the role of transport as a removal mechanism.

The TOMCAT runs *Control-NoDehydration* and *Hunga-NoDehydration* are similar to the standard runs but without the sedimentation of PSC particles. These

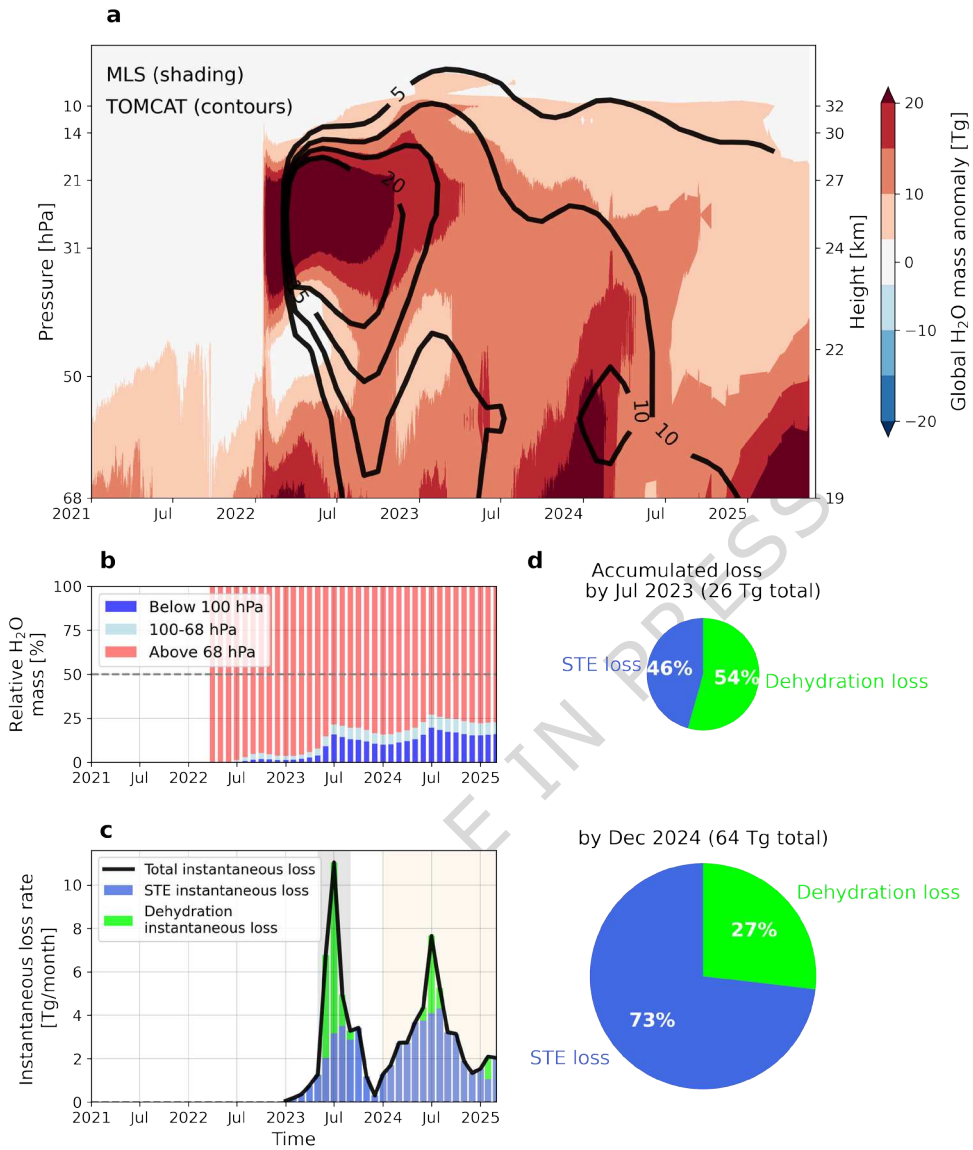

Fig. 3: Descent of Hunga excess H_2O to the lower stratosphere and subsequent loss in 2024 from MLS observations and TOMCAT model simulations. (a) Pressure-time cross section of MLS-observed (shading) daily global stratospheric H_2O mass anomalies, at each MLS layer, over January 2021 to June 2025 relative to the 2005–2021 climatology, together with TOMCAT model simulated (contours) monthly Hunga H_2O mass anomaly at each MLS layer. (b) Model-simulated relative distribution of the Hunga excess H_2O above (i.e., at pressures lower than) 68 hPa (red), over 100-68 hPa (light blue), and below (i.e., at pressures greater than) 100 hPa (blue), shown as stacked bars totaling 100%. (c) Time series showing the breakdown of Hunga H_2O total instantaneous loss (black line) into STE instantaneous loss (blue) and dehydration loss (lime). The grey and light yellow bars, similar to those in Fig. 1, mark the months of June and July 2023, and the year 2024, respectively. (d) The breakdown of Hunga H_2O cumulative loss into STE and dehydration components by July 2023 and December 2024, with the latter including removal during 2023. The 2024 loss on its own can be estimated by adding the blue bars during 2024 in panel (c). The attributions in (c) and (d) are obtained by comparing TOMCAT model simulations with and without PSC sedimentation.

runs allow us to diagnose the instantaneous (Fig. 3c) and accumulated (Fig. 3d) loss of HEW into contributions from the two processes, PSC sedimentation and STE. The relative contributions of the two processes change rapidly after the Antarctic PSC dehydration in 2023. The simulations without dehydration indicate that further removal of HEW by STE began in late 2023 and accelerated through 2024 (Fig. 3c). The timing is in agreement with the arrival of HEW in the lower stratosphere (Fig. 3b) via the slow BDC. This implies that the average removal rate by STE is ultimately determined by the rate at which the BDC transports mass from the overworld into the lowermost stratosphere. The fact that our simulated dehydration loss and the descending rate of HEW agree well with the observations demonstrates again that the model reproduces well the removal pathways of HEW. Although dehydration played a larger role than STE in reducing water vapour in July 2023, STE exceeded dehydration and became dominant by the end of 2024 (Fig. 3d). The model simulations indicate that both STE and Antarctic PSC dehydration will determine the removal of HEW for the coming years.

The mechanisms which destroy water vapour in the mesosphere act mostly at altitudes above 1 hPa. However, the mesospheric mass only increased by less than 2.5 Tg in the year 2024 as observed by MLS (Supplementary Fig. 3), accounting for only a small fraction (less than 1.75%) of HEW.

3 Return time

There have been attempts in the past two years to simulate the evolution of water vapour injected into the stratosphere by Hunga by computing a linear fit [20], using a simplified 2-D model [40], applying complex chemistry-climate models [21, 42], or developing a theoretical model [41] in order to predict the near-term impacts of this volcanic eruption. However, with no significant decline during the first two years following the eruption, it was not possible to robustly constrain the lifetime of Hunga H_2O using observations (see also Section 5.4 and Supplementary Fig.4). Many chemistry-climate models capture well the initial confinement above 25 km and subsequent large-scale evolution of Hunga H_2O, but overestimate the magnitude of Antarctic dehydration during the 2023 winter by a factor of 2–4 compared to MLS observations [21] because of deficiencies in their representations of PSC removal mechanisms or/and stratospheric transport. In contrast, our model calculations for Antarctic wintertime PSC sedimentation agree well with MLS observations as previously documented for 2023 [19] and further evaluated by the most recent drop in 2024 (Fig. 1). Thus, as shown in Fig. 4, we are able to estimate the decay time of Hunga excess H_2O with sufficient observational data to characterise the recent decay, along with model simulations that not only include realistic PSC dehydration loss but also take into account loss via stratosphere-to-troposphere transport by considering a longer post-eruption period with more realistic meteorological forcing than in the previous study using the same model [19].

By October 2023, MLS and TOMCAT are in close agreement (Fig. 1). After this point, the MLS time series briefly increases due to additional H_2O entering through the tropical tropopause, whereas the model remains unaffected and therefore represents

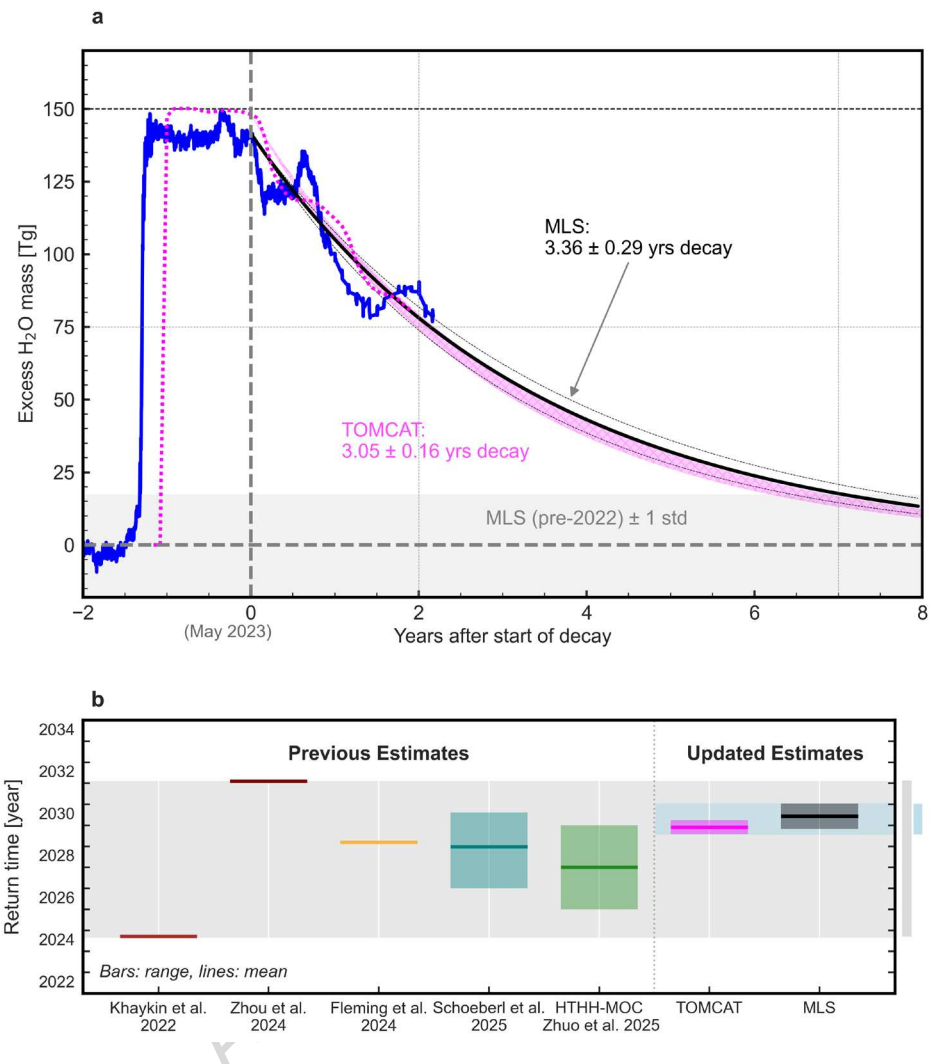

Fig. 4: **Decay and return time of global Hunga H_2O mass.** (a) The exponential decay of Hunga excess H_2O mass (Tg) applied to MLS (black, 3.36±0.13 years) and TOMCAT simulations (magenta, 3.05±0.16 years). The blue and magenta lines are the same as the timeseries shown in Figure 1. The light grey band near zero shows pre-Hunga natural variability (±1 standard deviations of pre-2022 MLS observations). (b) Updated estimates of return year (when stratospheric H_2O falls below pre-Hunga variability) compared with previous studies [19–21, 40, 41]. Return times from previous studies are recomputed by digitizing published figures. Bars indicate range where available and horizontal lines show mean values. Grey and blue bars on the right indicate the range from previous studies and our updated estimates, respectively.

HEW alone (see Section 5.3 for details). The drop then becomes steeper when efficient STE starts in 2024. Based on observations and simulations through early 2025, the current e-folding decay time of Hunga H_2O is ∼3 years (3.36±0.29 years for MLS; 3.05±0.15 years for model calculations) from the onset of the first removal when PSCs are formed in May 2023. This behaviour is consistent with a recent theoretical study on calculating the lifetime of various stratospheric constituents [43]. That study showed that the total lifetime (lag time + decay time) is less sensitive to the choice of the decay-onset date and thus enables more robust comparisons from different studies than simply using the e-folding time since start of removal alone. Results of such an intercomparison of estimated total lifetimes for HEW are shown in Supplementary Table 2. From May 2023, the half-life is ∼2 years, with 75 Tg being already removed from the stratosphere at the present time. After seven years of decay, both MLS-based estimation and the model simulations (Fig. 4a) show the excess H_2O burden dropping to the background variability (one standard deviation of MLS measurements over the pre-Hunga period; ∼ ±17 Tg), indicating the return of stratospheric water vapour abundances to the pre-Hunga level around the year 2030 (Fig. 4b).

4 Conclusions

MLS observations and TOMCAT model simulations have revealed remarkable change in decay pattern of Hunga-injected stratospheric H_2O from 2024 through early 2025. Dehydration in the 2023 Antarctic polar vortex caused the first substantial removal of Hunga H_2O from the stratosphere. However, with the H_2O gradually descending into the lower stratosphere via the slow BDC, transport into the troposphere becomes possible and H_2O is therefore removed more rapidly than it would be by dehydration alone. With sufficient observations from MLS and a model that reproduces transport well, our updated estimates of the residence time of the Hunga excess H_2O (with e-folding time of ∼3 years and a total lifetime of ∼4.5 years) substantially reduces the previous uncertainty (Fig. 4b) in predicting the fate of the Hunga H_2O.

5 Methods

5.1 MLS data

The Microwave Limb Sounder (MLS) instrument [22] was launched on NASA's Aura satellite in 2004. The field of view of the instrument is scanned vertically across the Earth's limb every ∼25 s, typically giving 3495 limb scans per day. The Aura orbit is inclined at 98°, and the instrument view is directed forward along the orbit plane, giving coverage from 82 °S to 82 °N each day. The horizontal resolution is about 1.5° along the orbit track. The orbit tracks are separated by about 25° at the equator, with closer longitudinal spacing at higher latitudes.

The water vapour measurement is made using the 183.3 GHz spectral line. The vertical resolution is about 3 km in the stratosphere and lower mesosphere. We use version 5 of the water vapour data [44]. A variety of changes have occurred between version 2 [45, 46] and version 5, and the improvements have been documented[44, 47].

For this study the MLS data (which cover the range 82°S–82°N) are averaged into daily zonal means in 5° latitude bins. Profiles that fail the recommended quality screening criteria [44] are discarded.

In 2024 it was discovered that the 190 GHz radiometer, which contains the channels used for the stratospheric H_2O measurement, was failing in a manner that would limit the total number of days for which it could be operated. In order to produce some water vapour data up to the end of the mission, the 190 GHz radiometer has been operated for only $\sim$ 7 days per calendar month, starting late in April 2024.

5.2 TOMCAT model and experiments

TOMCAT is a global three-dimensional (3-D) off-line chemical transport model (CTM) [25]. The model has been widely used for many studies of atmospheric chemistry and transport, particularly in the stratosphere. In the version used here, the large-scale meteorology is provided by vorticity, divergence, temperature and surface pressure fields from meteorological (re)analyses. Large-scale vertical motion is diagnosed on the model grid from the divergence. The model contains a detailed treatment of stratospheric chemistry, including the formation of polar stratospheric clouds, based on equilibrium occurrence.

For this study TOMCAT was integrated in a series of four experiments forced by ERA5 [26] meteorology. The model used a horizontal grid of 2.8° $\times$ 2.8° with 32 levels from the surface to about 60 km. Simulation *Control* was integrated from 1979 until 2025 using the standard model setup but without any additional treatment of Hunga. Simulation *Hunga* was initialised from simulation *Control* in January 2022 and included injection of 150 Tg H_2O from Hunga. This was added to the model in April 2022, by which point the water vapour had spread zonally and latitudinally [19]. Simulation *Control-NoDehydration* was the same as run *Control* except that sedimentation of PSCs was excluded after January 2022. Similarly, *Hunga-NoDehydration* was identical to *Hunga* but again without sedimentation of PSCs. These two sets of paired runs were used to diagnose the changes of HEW. The difference between the HEW time series in each pair isolates the contribution from polar PSC dehydration, and the remaining loss is attributed to STE.

5.3 Calculating H_2O mass

MLS H_2O anomalies are calculated as deviations from the 2005–2021 climatology. In Figure 2, we applied a 15-day running mean to minimize the gaps present in the MLS data since April 2024 (shown in green and red lines of Figs. 2b, 2d), which resulted from the "one week in four" operation of MLS. In all other figures, raw (unsmoothed) anomalies are shown. The model anomalies are calculated as differences between runs *Hunga* and *Control*. The stratospheric total mass of H_2O is estimated for pressure levels above 68 hPa. For MLS, it is calculated as the global (82°S-82°N) sum of the stratospheric column over each 5-degree latitude band from MLS volume mixing ratio measurements from 68 hPa to $\sim$0.4 hPa. The modelled stratospheric H_2O total mass is calculated as the sum of the H_2O mass in each grid box from 68 hPa to the model top ($\sim$0.2 hPa). We used 68 hPa rather than 100 hPa to avoid the

influence of additional water vapour from the troposphere. The model simulations are not affected by the additional H_2O entry as it uses a fixed repeating seasonal cycle of H_2O tropical entry. For example, the large increase in MLS global stratospheric H_2O from late 2023 to early 2024 arises from anomalously enhanced H_2O entry through the tropical tropopause, whereas TOMCAT does not include this interannual variability and therefore reflects only the Hunga-caused excess (Fig. 1). The amount of HEW over 100-68 hPa is stable (∼10 Tg; see Fig. 3b light-blue shading) in year 2024, therefore using 100 hPa for the model makes little difference. Polar cap averages are computed as the mean over latitudes poleward of 70°S and 70°N.

5.4 Uncertainty estimation for the decay time

The uncertainty in the e-folding decay time was quantified using both the formal fitting uncertainty and the spread arising from natural variability. We applied a nonlinear least-squares fit in SciPy [48] to the HEW time series through July 2025. Assuming exponential decay, we obtained an e-folding decay time of 3.36 years for MLS and a two-sigma fitting error of approximately 0.13 years. To verify the fitting error, we performed a Monte-Carlo resampling and obtained a posterior distribution with a similar two-sigma spread (∼0.12 years), confirming the robustness of the fit-based estimate. The MLS time series, however, is also influenced by natural variability (see Section 5.3), which should also be accounted for in the uncertainty estimation. We examined the evolution of the fitted decay time as the observational record lengthened (see Supplementary Fig. 4). After one year of the decay, the inferred decay time becomes stable, giving a variability-driven two-sigma spread of ∼0.26 years. Combining the variability-driven spread and fitting uncertainty in quadrature (by taking the square root of the sum of the squares of uncertainties), we obtain a total uncertainty of ∼0.29 years for MLS.

Data availability

MLS satellite data, including the version 5 H_2O data used in this paper [49], are publicly available at https://disc.gsfc.nasa.gov. TOMCAT model outputs are available on request from the corresponding authors. All of the pre-processed model data (for example, monthly mean water vapour mass averaged globally and over Antarctica from TOMCAT and water vapour mass interpolated onto the MLS vertical coordinates) are available at Zenodo (https://doi.org/10.5281/zenodo.18193651) [50].

Supplementary information. This file contains Supplementary Figs. 1–4 and Supplementary Tables 1–2.

Acknowledgements. XZ and QC acknowledge funding from the National Natural Science Foundation of China (U2442210, 42275059, 12411530093). MPC and SSD were supported by the NCEO TerraFIRMA, NERC LSO3 (NE/V011863/1) and ESA OREGANO (4000137112/22/I-AG) projects. The TOMCAT model simulations were performed on the UK Archer2 and Leeds ARC HPC systems. Work at the Jet Propulsion Laboratory, California Institute of Technology, was carried out under a contract with the National Aeronautics and Space Administration (80NM0018D0004).

Competing interests. The authors declare no competing interests.

Code availability. Code from the TOMCAT CTM is available on suitable request from Martyn Chipperfield. The code used to generate all of the figures in this analysis is available at Zenodo (https://doi.org/10.5281/zenodo.18193651) [50].

Author contribution. X.Z. and M.P.C. designed the study. M.P.C., X.Z., and W.F. designed and performed TOMCAT simulations. X.Z. analysed the data and produced the figures. X.Z., M.P.C., and H.C.P. drafted the initial text. S.S.D., S.H., G.M., L.M., M.L.S. and Q.C. contributed substantially to the interpretation of findings.

References

[1] Forster, P. M. d. F. & Shine, K. P. Assessing the climate impact of trends in stratospheric water vapor. *Geophysical Research Letters* **29**, 10–1–10–4 (2002).

[2] Solomon, S. *et al.* Contributions of stratospheric water vapor to decadal changes in the rate of global warming. *science* **327**, 1219–1223 (2010).

[3] Millán, L. *et al.* Hunga Tonga-Hunga Ha'apai hydration of the stratosphere. *Geophys. Res. Lett* **49**, e2022GL099381 (2022).

[4] Evan, S. *et al.* Rapid ozone depletion after humidification of the stratosphere by the Hunga Tonga Eruption. *Science* **382**, eadg2551 (2023).

[5] Santee, M. L. *et al.* Strong evidence of heterogeneous processing on stratospheric sulfate aerosol in the extrapolar Southern Hemisphere following the 2022 Hunga Tonga-Hunga Ha'apai eruption. *Journal of Geophysical Research: Atmospheres* **128**, e2023JD039169 (2023).

[6] Wilmouth, D. M., Østerstrøm, F. F., Smith, J. B., Anderson, J. G. & Salawitch, R. J. Impact of the Hunga Tonga volcanic eruption on stratospheric composition. *Proceedings of the National Academy of Sciences* **120**, e2301994120 (2023).

[7] Zhu, Y. *et al.* Perturbations in stratospheric aerosol evolution due to the water-rich plume of the 2022 Hunga-Tonga eruption. *Communications Earth & Environment* **3**, 248 (2022).

[8] Coy, L. *et al.* Stratospheric circulation changes associated with the Hunga Tonga-Hunga Ha'apai eruption. *Geophysical Research Letters* **49**, e2022GL100982 (2022).

[9] Schoeberl, M. R. *et al.* Analysis and impact of the Hunga Tonga-Hunga Ha'apai stratospheric water vapor plume. *Geophysical Research Letters* **49**, e2022GL100248 (2022).

[10] Sellitto, P. *et al.* The unexpected radiative impact of the Hunga Tonga eruption of 15th January 2022. *Communications Earth & Environment* **3**, 288 (2022).

[11] Yu, W. *et al.* Mesospheric temperature and circulation response to the Hunga Tonga-Hunga-Ha'apai volcanic eruption. *Journal of Geophysical Research: Atmospheres* **128**, e2023JD039636 (2023).

[12] Jenkins, S., Smith, C., Allen, M. & Grainger, R. Tonga eruption increases chance of temporary surface temperature anomaly above 1.5 °C. *Nature Climate Change* **13**, 127–129 (2023).

[13] Schoeberl, M. R. *et al.* Evolution of the climate forcing during the two years after the hunga tonga-hunga ha'apai eruption. *Journal of Geophysical Research: Atmospheres* **129**, e2024JD041296 (2024).

[14] Stenchikov, G., Ukhov, A. & Osipov, S. Modeling the radiative forcing and atmospheric temperature perturbations caused by the 2022 hunga volcano explosion. *Journal of Geophysical Research: Atmospheres* **130**, e2024JD041940 (2025).

[15] Vömel, H., Oltmans, S., Hofmann, D., Deshler, T. & Rosen, J. The evolution of the dehydration in the Antarctic stratospheric vortex. *Journal of Geophysical Research: Atmospheres* **100**, 13919–13926 (1995).

[16] Holton, J. R. *et al.* Stratosphere-troposphere exchange. *Reviews of Geophysics* **33**, 403–439 (1995).

[17] Nedoluha, G. E. *et al.* Water vapor measurements in the mesosphere from Mauna Loa over solar cycle 23. *Journal of Geophysical Research: Atmospheres* **114** (2009).

[18] Millán, L. *et al.* The evolution of the Hunga hydration in a moistening stratosphere. *Geophysical Research Letters* **51**, e2024GL110841 (2024).

[19] Zhou, X. *et al.* Antarctic vortex dehydration in 2023 as a substantial removal pathway for Hunga Tonga-Hunga Ha'apai water vapor. *Geophysical Research Letters* **51**, e2023GL107630 (2024).

[20] Khaykin, S. *et al.* Global perturbation of stratospheric water and aerosol burden by Hunga eruption. *Communications Earth & Environment* **3**, 316 (2022).

[21] Zhuo, Z. *et al.* Comparing multi-model ensemble simulations with observations and decadal projections of upper atmospheric variations following the hunga eruption. *Atmospheric Chemistry and Physics* **25**, 13161–13176 (2025).

[22] Waters, J. W. *et al.* The Earth Observing System Microwave Limb Sounder (EOS MLS) on the Aura satellite. *IEEE Trans. Geoscience and Remote Sensing* **44**, 1106–1121 (2006).

[23] Randel, W. J., Wu, F., Vömel, H., Nedoluha, G. E. & Forster, P. Decreases in stratospheric water vapor after 2001: Links to changes in the tropical

tropopause and the Brewer-Dobson circulation. *Journal of Geophysical Research: Atmospheres* **111**, D2312 (2006).

[24] Urban, J., Lossow, S., Stiller, G. & Read, W. Another drop in water vapor. *Eos, Transactions American Geophysical Union* **95**, 245–246 (2014).

[25] Chipperfield, M. New version of the TOMCAT/SLIMCAT off-line chemical transport model: Intercomparison of stratospheric tracer experiments. *Quarterly Journal of the Royal Meteorological Society: A journal of the atmospheric sciences, applied meteorology and physical oceanography* **132**, 1179–1203 (2006).

[26] Hersbach, H. *et al.* The ERA5 global reanalysis. *Quarterly Journal of the Royal Meteorological Society* **146**, 1999–2049 (2020).

[27] Mote, P. W. *et al.* An atmospheric tape recorder: The imprint of tropical tropopause temperatures on stratospheric water vapor. *Journal of Geophysical Research: Atmospheres* **101**, 3989–4006 (1996).

[28] Manney, G. L. *et al.* Siege in the southern stratosphere: Hunga Tonga-Hunga Ha'apai water vapor excluded from the 2022 Antarctic polar vortex. *Geophysical Research Letters* **50**, e2023GL103855 (2023).

[29] Santee, M. L. *et al.* The influence of stratospheric hydration from the hunga eruption on chemical processing in the 2023 Antarctic vortex. *Journal of Geophysical Research: Atmospheres* **129**, e2023JD040687 (2024).

[30] Wohltmann, I., Santee, M. L., Manney, G. L. & Millán, L. F. The chemical effect of increased water vapor from the Hunga Tonga-Hunga Ha'apai eruption on the Antarctic ozone hole. *Geophysical Research Letters* **51**, e2023GL106980 (2024).

[31] Pitts, M. C., Poole, L. R., Dörnbrack, A. & Thomason, L. W. The 2009–2010 Arctic polar stratospheric cloud season: a CALIPSO perspective. *Atmospheric Chemistry and Physics* **11**, 2161–2177 (2011).

[32] Khaykin, S. M. *et al.* Arctic stratospheric dehydration–part 1: Unprecedented observation of vertical redistribution of water. *Atmospheric Chemistry and Physics* **13**, 11503–11517 (2013).

[33] Manney, G. L. & Lawrence, Z. D. The major stratospheric final warming in 2016: dispersal of vortex air and termination of Arctic chemical ozone loss. *Atmospheric Chemistry and Physics* **16**, 15371–15396 (2016).

[34] Manney, G. L. *et al.* Record-low Arctic stratospheric ozone in 2020: MLS observations of chemical processes and comparisons with previous extreme winters. *Geophysical Research Letters* **47**, e2020GL089063 (2020).

[35] Newman, P. A. *et al.* Record high March 2024 Arctic total column ozone. *Geophysical Research Letters* **51**, e2024GL110924 (2024).

[36] Lee, S. H., Butler, A. H. & Manney, G. L. Two major sudden stratospheric warmings during winter 2023/2024. *Weather* **80**, 45–53 (2025).

[37] Basha, G. *et al.* Impact of Hunga Tonga-Hunga Ha'apai volcanic eruption on stratospheric water vapour, temperature, and ozone. *Remote Sensing* **15**, 3602 (2023).

[38] Nedoluha, G. E. *et al.* The spread of the Hunga Tonga H_2O plume in the middle atmosphere over the first two years since eruption. *Journal of Geophysical Research: Atmospheres* **129**, e2024JD040907 (2024).

[39] Manney, G. L., Zurek, R. W., O'Neill, A. & Swinbank, R. On the motion of air through the stratospheric polar vortex. *Journal of Atmospheric Sciences* **51**, 2973 – 2994 (1994).

[40] Fleming, E. L., Newman, P. A., Liang, Q. & Oman, L. D. Stratospheric temperature and ozone impacts of the Hunga Tonga-Hunga Ha'apai water vapor injection. *Journal of Geophysical Research: Atmospheres* **129**, e2023JD039298 (2024).

[41] Schoeberl, M. R., Toohey, M., Wang, Y. & Ueyama, R. Stratospheric injection lifetimes. *Journal of Geophysical Research: Atmospheres* **130**, e2025JD043928 (2025).

[42] Kuchar, A. *et al.* Modulation of the northern polar vortex by the Hunga Tonga–Hunga Ha'apai eruption and the associated surface response. *Atmospheric Chemistry and Physics* **25**, 3623–3634 (2025).

[43] Toohey, M., Jia, Y., Khanal, S. & Tegtmeier, S. Stratospheric residence time and the lifetime of volcanic stratospheric aerosols. *Atmospheric Chemistry and Physics* **25**, 3821–3839 (2025).

[44] Livesey, N. J. *et al.* Earth Observing System (EOS) Aura Microwave Limb Sounder (MLS) version 5.0x level 2 and 3 data quality and description document. Tech. Rep. JPL D-105336 Rev. B, NASA Jet Propulsion Laboratory California Institute of Technology, Pasadena, California, 91109-8099 (2022). URL https://mls.jpl.nasa.gov.

[45] Lambert, A. *et al.* Validation of the Aura Microwave Limb Sounder middle atmosphere water vapor and nitrous oxide measurements. *J. Geophys. Res* **112**, D24S35 (2007).

[46] Khosrawi, F. *et al.* The SPARC water vapour assessment II: comparison of stratospheric and lower mesospheric water vapour time series observed from satellites. *Atmospheric Measurement Techniques* **11**, 4435–4463 (2018).

[47] Livesey, N. J. *et al.* Investigation and amelioration of long-term instrumental drifts in water vapor and nitrous oxide measurements from the Aura Microwave Limb Sounder (MLS) and their implications for studies of variability and trends. *Atmospheric Chemistry and Physics* **21**, 15409–15430 (2021).

[48] Virtanen, P. *et al.* SciPy 1.0: fundamental algorithms for scientific computing in Python. *Nature methods* **17**, 261–272 (2020).

[49] Lambert, A., Read, W. & Livesey, N. MLS/Aura level 2 water vapor (H2O) mixing ratio v005 (2020). Accessed 2025-07-28.

[50] Zhou, X. Data and code for "Residence time of Hunga stratospheric water vapour perturbation quantified at 9 years" [data set]. *Zendo* (2025). URL https://doi.org/10.5281/zenodo.18193651.

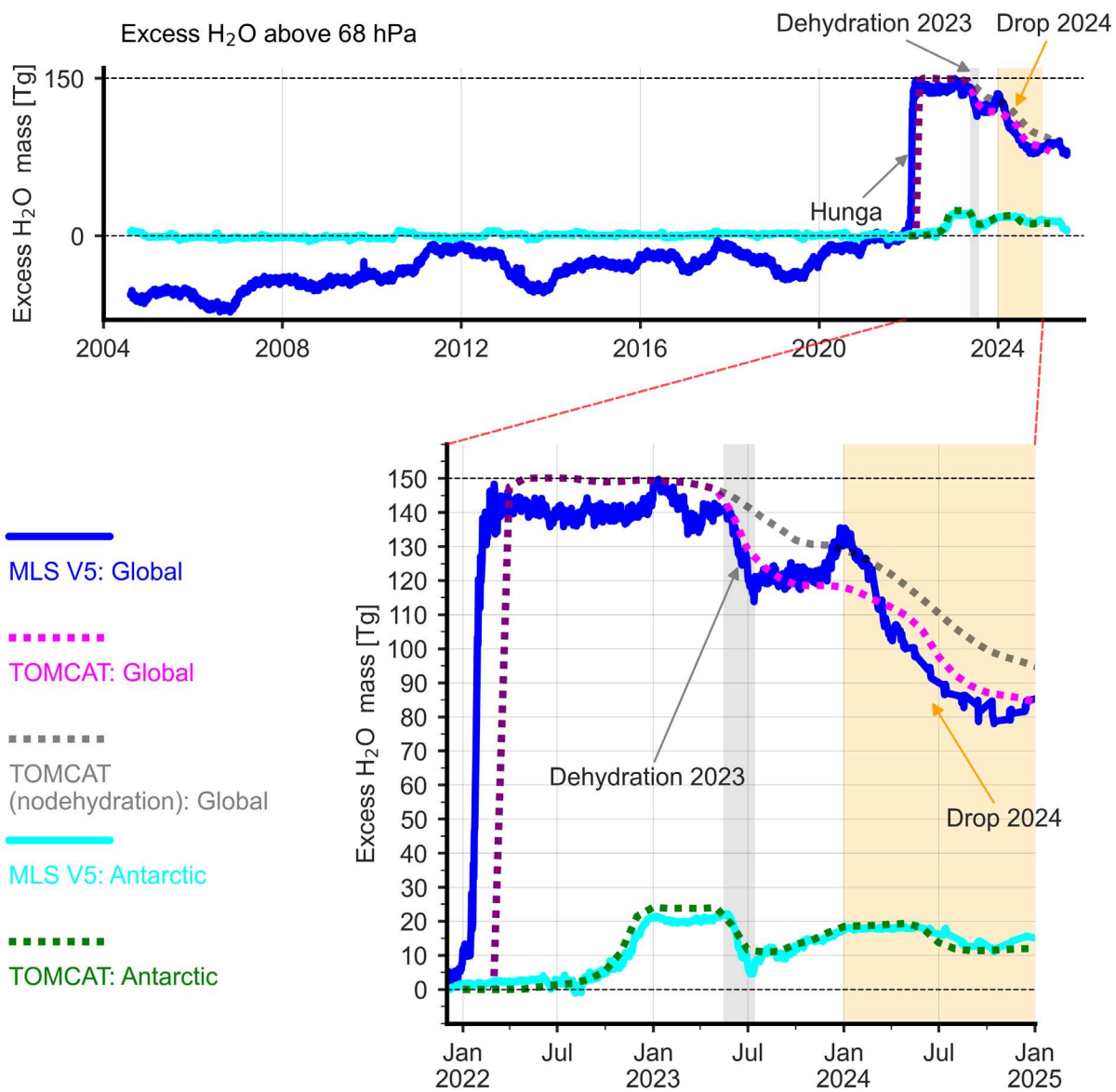
Excess H_2O above 68 hPa
Dehydration 2023
Drop 2024
Hunga
Excess H_2O mass [Tg]
150
0
2004
2008
2012
2016
2020
2024
MLS V5: Global
TOMCAT: Global
TOMCAT (nodehydration): Global
MLS V5: Antarctic
TOMCAT: Antarctic
Excess H_2O mass [Tg]
150
140
130
120
110
100
90
80
70
60
50
40
30
20
10
0
Dehydration 2023
Drop 2024
Jan 2022
Jul
Jan 2023
Jul
Jan 2024
Jul
Jan 2025

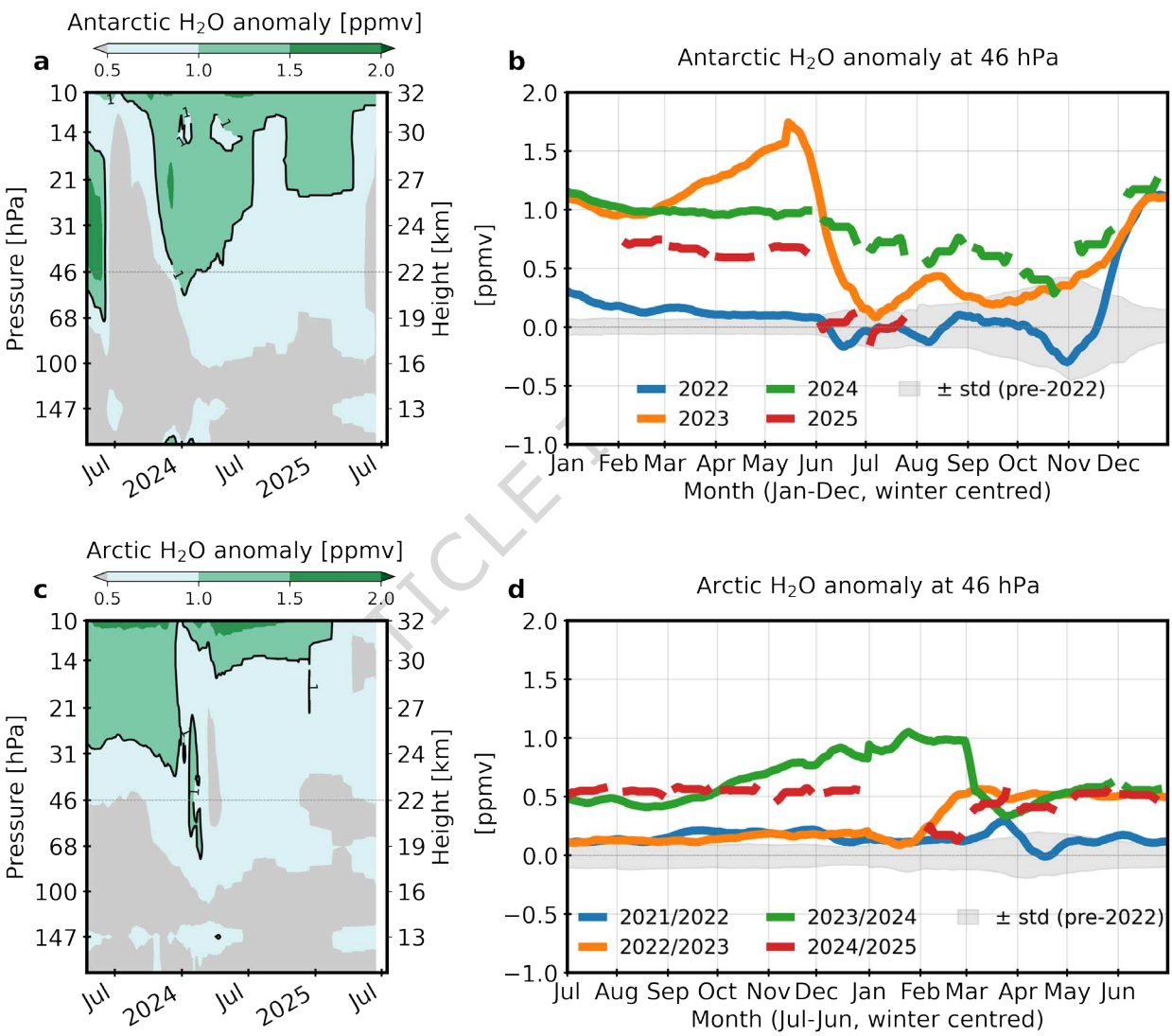
a
Antarctic H2O anomaly [ppmv]
0.5
1.0
1.5
2.0
Pressure [hPa]
Height [km]
10
14
21
31
46
68
100
147
32
30
27
24
22
19
16
13
Jul
2024
Jul
2025
Jul
b
Antarctic H2O anomaly at 46 hPa
[ppmv]
2.0
1.5
1.0
0.5
0.0
−0.5
−1.0
2022
2023
2024
2025
± std (pre-2022)
Jan Feb Mar Apr May Jun Jul Aug Sep Oct Nov Dec
Month (Jan-Dec, winter centred)
c
Arctic H2O anomaly [ppmv]
0.5
1.0
1.5
2.0
Pressure [hPa]
Height [km]
10
14
21
31
46
68
100
147
32
30
27
24
22
19
16
13
Jul
2024
Jul
2025
Jul
d
Arctic H2O anomaly at 46 hPa
[ppmv]
2.0
1.5
1.0
0.5
0.0
−0.5
−1.0
2021/2022
2022/2023
2023/2024
2024/2025
± std (pre-2022)
Jul Aug Sep Oct Nov Dec Jan Feb Mar Apr May Jun
Month (Jul-Jun, winter centred)

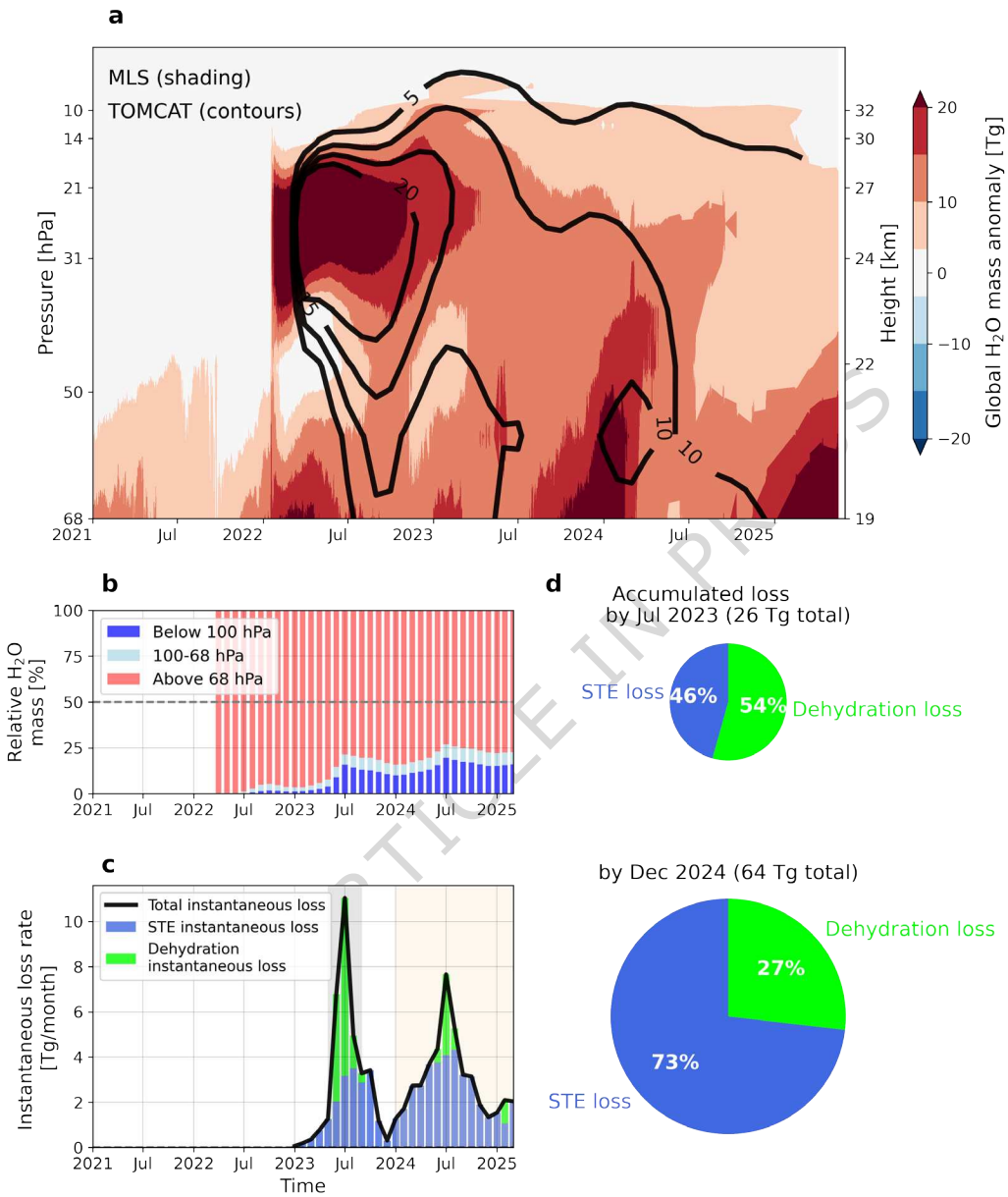
a
MLS (shading)
TOMCAT (contours)
Pressure [hPa]
Height [km]
Global H2O mass anomaly [Tg]
b
Relative H2O mass [%]
Below 100 hPa
100-68 hPa
Above 68 hPa
c
Instantaneous loss rate [Tg/month]
Total instantaneous loss
STE instantaneous loss
Dehydration instantaneous loss
Time
d
Accumulated loss by Jul 2023 (26 Tg total)
STE loss 46%
54% Dehydration loss
by Dec 2024 (64 Tg total)
Dehydration loss 27%
73% STE loss

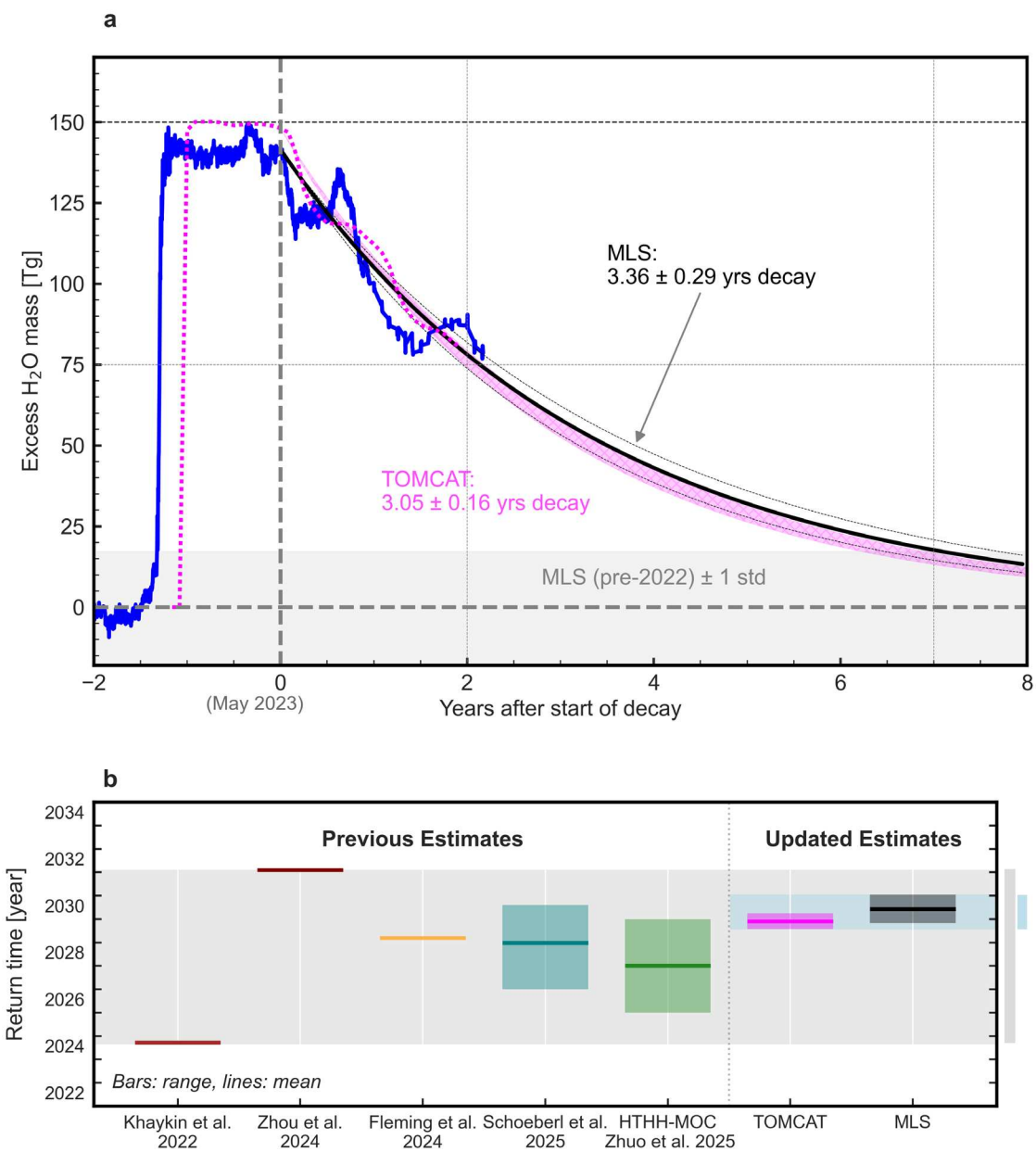
a
Excess H_2O mass [Tg]
150
125
100
75
50
25
0
MLS:
3.36 ± 0.29 yrs decay
TOMCAT:
3.05 ± 0.16 yrs decay
MLS (pre-2022) ± 1 std
−2
0
(May 2023)
2
4
6
8
Years after start of decay
b
Return time [year]
2034
2032
2030
2028
2026
2024
2022
Previous Estimates
Updated Estimates
Bars: range, lines: mean
Khaykin et al. 2022
Zhou et al. 2024
Fleming et al. 2024
Schoeberl et al. 2025
HTHH-MOC Zhuo et al. 2025
TOMCAT
MLS